

A polarization system for persistent chemical detection

Julia Craven-Jones¹, Leah Appelhans¹, Eric Couphos¹, Todd Embree¹, Patrick Finnegan¹, Dennis Goldstein², David Karelitz¹, Charles LaCasse¹, Ting S. Luk¹, Adoum Mahamat³, Lee Massey¹, Anthony Tanbakuchi¹, Cody Washburn¹, Steven Vigil¹

¹Sandia National Laboratories, 1515 Eubank Blvd SE, Albuquerque, NM 87123

²Polaris Sensor Technologies, 200 West Court Square Suite 320, Huntsville, AL 35801

³College of Optical Sciences, University of Arizona, Tucson, AZ 85721

ABSTRACT

We report on the development of a prototype polarization tag based system for detecting chemical vapors. The system primarily consists of two components, a chemically sensitive tag that experiences a change in its optical polarization properties when exposed to a specific chemical of interest, and an optical imaging polarimeter that is used to measure the polarization properties of the tags. Although the system concept could be extended to other chemicals, for the initial system prototype presented here the tags were developed to be sensitive to hydrogen fluoride (HF) vapors. HF is used in many industrial processes but is highly toxic and thus monitoring for its presence and concentration is often of interest for personnel and environmental safety. The tags are periodic multilayer structures that are produced using standard photolithographic processes. The polarimetric imager has been designed to measure the degree of linear polarization reflected from the tags in the short wave infrared. By monitoring the change in the reflected polarization signature from the tags, the polarimeter can be used to determine if the tag was exposed to HF gas. In this paper, a review of the system development effort and preliminary test results are presented and discussed, as well as our plan for future work.

Keywords: chemical detection, chemical sensing, gas detection, polarization tag, hydrogen fluoride sensing

1. INTRODUCTION

Hazardous chemical detection is a necessary monitoring capability for a variety of industrial and manufacturing processes, especially for facilities where exposure monitoring is crucial to ensuring a safe workplace and minimizing environmental impact. Consequently, the development of low concentration chemical detectors and monitors is an active area of research. A number of chemical monitoring systems are commercially available, and several groups are pursuing novel approaches to hazardous gas detection [1-5].

Many of the currently available commercial approaches for chemical monitoring are based on active detection systems that must be powered by a battery or a wall outlet for the entirety of their use. These systems can be impressively sensitive (down to the parts-per-billion, or ppb, level for some chemicals) and can deliver analysis results quickly. However, requiring an active power supply for operation may limit the usefulness of this type of monitoring approach in some situations, including emergencies. Alternatively, passive detection technologies do not require power during monitoring and are typically based on a total-dose measurement over an extended period of time. For these types of sensors, the dosimeter is either placed in the area to be monitored or worn by an individual for a predetermined period of time, after which the dosimeter is analyzed. Regularly, this analysis occurs at an external laboratory, and feedback on the results can be delayed by several days.

This paper presents results from the development of a prototype polarization tag based chemical monitoring system (PChemS) designed to monitor an area for the presence of a hazardous chemical. Although the system concept could be extended to other chemicals, for the initial system prototype presented here the monitoring tags were developed to indicate exposure to hydrogen fluoride (HF) gas. HF is used in many industrial processes but is highly toxic and thus monitoring for its presence and concentration is often of interest for personnel and environmental safety. The monitoring system primarily consists of two components. First, building on previous research into HF

sensitive tag development [6, 7], the system includes a chemically sensitive tag that experiences a change in its polarization properties when exposed to a specific chemical of interest. The tags are small (our prototypes have active areas of 1.0 or 2.5 centimeters square), low profile, and easily installed, and can be left unattended to monitor for extended periods. The second component of the system is a passive optical imaging polarimeter that is used to measure the polarization properties of light reflected off of the tags. Chemical detection occurs by comparing the linear polarization signature of light reflected off of the tag before and after the monitoring period using the polarimeter and a broadband low power illumination source. If the tag was exposed to detectable concentration of HF, a polarization change is observed (and the absence of change indicates no detectable exposure occurred).

Our approach of using a tag to generate a secondary polarization signature for a chemical such as HF that cannot be detected directly using polarimetry is fairly unconventional, but offers some unique advantages and capabilities over the current commercial state of the art. Unlike currently available commercial active monitoring systems, the polarization tag presented here is completely passive and requires no power or other support during its monitoring period; however unlike current passive approaches, by incorporating a field portable analyzer in the form of an optical polarimeter, our system enables analysis to be performed in situ and results to be obtained nearly immediately. Additionally, while active commercial systems use techniques such as spectroscopy to probe for unique and potentially very faint and fleeting chemical signatures, detection in our approach is based on permanent optical material property changes induced by a chemical reaction. Thus, this detection mechanism enables persistent monitoring without the need for persistent presence or active monitoring.

Our work was primarily focused on realizing a proof of concept monitoring system based on this polarization tag based detection approach, and this paper presents the major results of this effort. Specifically, section 2 provides more details of our approach and the relevant underlying polarimetric theory. System development, including development of both the polarization tags as well as the polarimeter, is presented in section 3. In addition, demonstrating this monitoring concept required some testing of the HF concentrations and exposure conditions that could be detected using the prototype system, and our results from this testing are presented in section 4. Finally, section 5 summarizes our conclusions and our plans for future work.

2. APPROACH

Figure 1 illustrates the envisioned implementation of the tag based chemical monitoring system. Based on anticipated user needs, the overall application of the system is anticipated to be indoor monitoring, and the monitoring tags would be installed in one or more locations for periods of weeks to months at a time. There are three focal points of the system: the chemically sensitive tags, which experience a change in optical properties when exposed to the chemical of interest, the polarimeter, which is used to measure the polarization properties of light reflected off of tags (from a distance of approximately 0.5-10 m), and the operational environment including the illumination source and the ambient atmosphere. We assume that a broadband low power light source with constant polarization properties, such as an incandescent lamp, serves as the illumination source for our system, and that the atmosphere does not induce any changes in the polarization properties of light emanating from the source and incident on the tag or received at the polarimeter upon reflection off of the tag.

We use the Stokes-Mueller formalism [8] to describe the interaction of partially polarized and incoherent light with a medium such that the incident light, represented as a vector, is modified by the characteristics of the medium, represented by a matrix. The result of this interaction is a vector that represents the modified light. The equation that describes this process is given as

$$\vec{S}_{out} = \begin{pmatrix} S_0 \\ S_1 \\ S_2 \\ S_3 \end{pmatrix}_{out} = \begin{pmatrix} m_{11} & m_{12} & m_{13} & m_{14} \\ m_{21} & m_{22} & m_{23} & m_{24} \\ m_{31} & m_{32} & m_{33} & m_{34} \\ m_{41} & m_{42} & m_{43} & m_{44} \end{pmatrix} \begin{pmatrix} S_0 \\ S_1 \\ S_2 \\ S_3 \end{pmatrix}_{in} = M\vec{S}_{in}. \quad (1)$$

The Mueller matrix M provides a complete polarimetric characterization of a sample and is implicitly dependent on wavelength, spatial coordinates, and illumination and observation geometries. The incident light is represented by the Stokes vector S . The Stokes vector consists of four Stokes parameters that are derived from a series of at least four intensity measurements at four polarizations. The elements of the Stokes vector are associated with total light

flux (S_0), linear polarization (S_1 and S_2) and circular polarization (S_3). If all four Stokes parameters are measured for a given spatial, spectral, and temporal coordinate, then the polarization state of the light emanating from that coordinate is fully characterized.

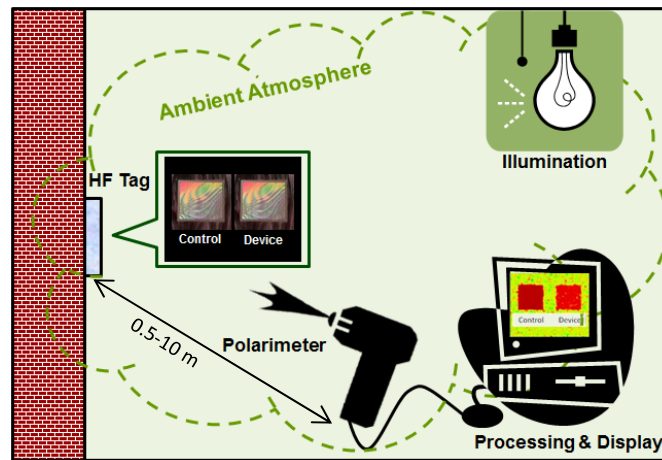


Figure 1. Diagram of the envisioned tag based monitoring system implementation.

If the polarimeter in our system measured M_{tag} for a given monitoring tag, the complete polarization properties of the tag would be known. Because M_{tag} is independent of the polarization properties of the illumination source, measuring M_{tag} is the most direct approach for characterizing the properties of a tag before and after a monitoring period. However, for the envisioned measurement scenario, the tags are illuminated by a source with a fixed input polarization state. Without the ability to actively vary the polarization properties of the source, the polarimeter is not capable of measuring M_{tag} directly, and must instead analyze the light reflected off of the tag, represented by the Stokes vector of this light, to determine if it was exposed to the chemical.

Although there are cases where individual Stokes parameters are of interest, our application is particularly interested in changes in overall degree of polarization (DOP), where

$$DOP = \frac{\sqrt{S_1^2 + S_2^2 + S_3^2}}{S_0}. \quad (2)$$

As reviewed in previous paragraphs, the anticipated implementation approach for the system leverages a low power broadband source to illuminate the tags. However, measurement of S_3 over broad wavelength ranges often requires custom achromatic retarder elements which can be difficult and costly to design and realize. Thus to simplify the tag measurement process, the geometry of the tag microstructure, discussed in more detail in a subsequent section, was designed to produce a primarily linear polarization signature. Under this constraint the degree of linear polarization ($DOLP$) can be used to as a single metric for monitoring with the tag system, where

$$DOLP = \frac{\sqrt{S_1^2 + S_2^2}}{S_0}. \quad (3)$$

Since S_1 and S_2 both quantify the linear polarization observed emanating from an object, $DOLP$ is a convenient metric for determining the overall linear polarization independent of orientation angle. Since it is normalized by S_0 , $DOLP$ values range from 0 (no linear polarization) to 1 (completely linearly polarized).

3. SYSTEM DEVELOPMENT

3.1 Tag Development

The tags developed for the chemical detection system are periodic structure based elements intended to simulate wire grid polarizers. They consist of a silicon-based structured tag substrate produced using standard photolithographic processes [6, 7, 9] and coated with a titanium dioxide HF-sensitive material. The period of the structure is nominally $2.3\ \mu\text{m}$ with a 50% duty cycle, and the depth of the grooves is nominally $5\ \mu\text{m}$. Figure 2 (a) presents an optical microscope photograph of the repeating tag substrate architecture, with relevant dimensions labeled. The tag design includes an overarching 'brick' structure to improve tag robustness and a higher spatial frequency periodic structure that is used to provide the polarimetric response. A cross-sectional scanning electron microscope (SEM) image of the periodic structure within a 'brick' is shown in Figure 2 (b). Typically, the tags were fabricated to have a $1\ \text{cm} \times 1\ \text{cm}$ active area, and approximately 12 tags were produced simultaneously on a standard 4 inch diameter silicon-on-insulator wafer, as depicted in Figure 3, which was then diced to produce individual tags. As also depicted in Figure 3, other tag sizes are possible and were demonstrated.

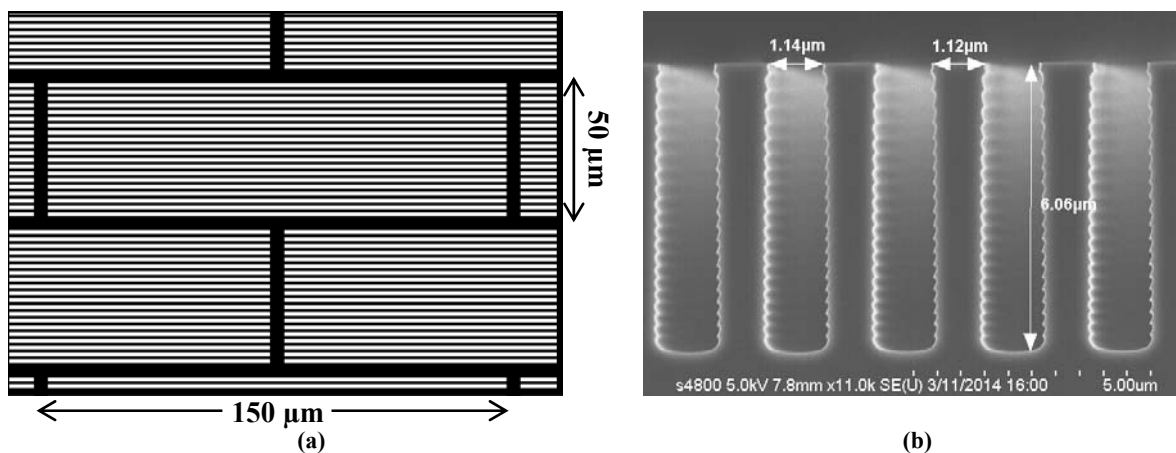


Figure 2. Tag substrate. (a) A small portion of the tag substrate structure, viewed from above. (b) A cross section of the tag structure.

Throughout the tag development process, a number of techniques for incorporating an HF sensitive material into the tag were developed and tested [7, 9]. Ultimately of all materials tested for this application, we identified amorphous titanium dioxide (TiO_2) deposited onto the tag substrates in a high vacuum electron-beam system as the incorporation (coating) approach that offered the most consistency, sensitivity, and selectivity. Evaporative deposition heats the TiO_2 to an evaporation point and is then allowed to cool and deposit on the surfaces of the periodic structure. A variety of TiO_2 coating thicknesses were tested, and our testing indicated that coating thicknesses of 100 nm or thicker provided the largest changes in polarimetric signatures after exposure to HF gas.

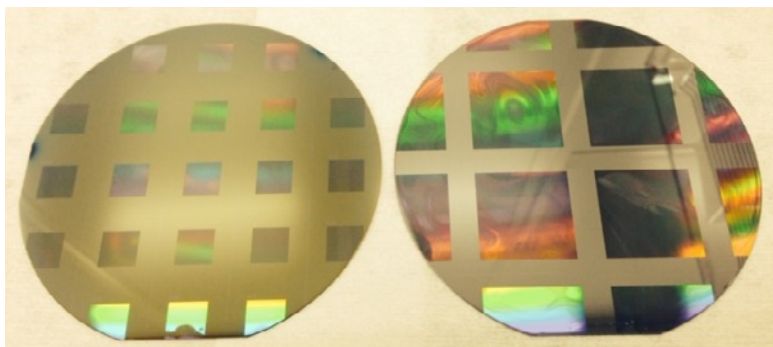


Figure 3. One centimeter and one inch tags patterned on 4 inch diameter silicon wafers.

Many material studies were performed as a part of the tag development process to understand the chemical and morphological effects of the reaction of HF gas with the TiO₂ tag coating (and other coating materials tested), including x-ray diffraction, x-ray photoelectron spectroscopy, and energy dispersive spectroscopy [9]. These techniques identified the probable product of TiO₂ exposure to HF as the hydronium titanium oxyfluoride phase (H₃O)_xTiO_yF_z which has previously been described in the literature [10].

However for the use of the tags as an optical based chemical detector, change in index of refraction of the tags after exposure to HF is one of the most important quantities to characterize and understand. To quantify these changes, ellipsometric data was acquired using unpatterned silicon wafers coated with thin films of the amorphous TiO₂ material used for the tags. A J.A. Woollam IR-VASE ellipsometer, which covers a spectral range of 250-6000 cm⁻¹ (or 40-1.67 μm) was used for the measurements. The ellipsometric samples were exposed to an HF concentration of 30 parts per million (ppm) for a period of 1 day at 30% relative humidity (RH) using the gaseous exposure system presented in section 3.2. The refractive index functions obtained from ellipsometric measurements of the sample both before and after the exposure are depicted in Figure 4. The real component of the refractive index of the exposed film in the 1250 - 5000 cm⁻¹ region ($\lambda = 2.0 - 8.0 \mu\text{m}$) is reduced significantly after exposure. In the spectral region of 250-1000 cm⁻¹ ($\lambda = 10 - 40 \mu\text{m}$), the absorption (imaginary part of the index of refraction) is also reduced significantly. These results suggest that the change in material properties that is observed in other techniques also manifests as changes in the optical constants of the product material, which should, when combined with the tag patterning, result in changes in the polarization properties of the tags after exposure to HF for infrared wavelengths $\lambda = 2.0 - 12.0 \mu\text{m}$.

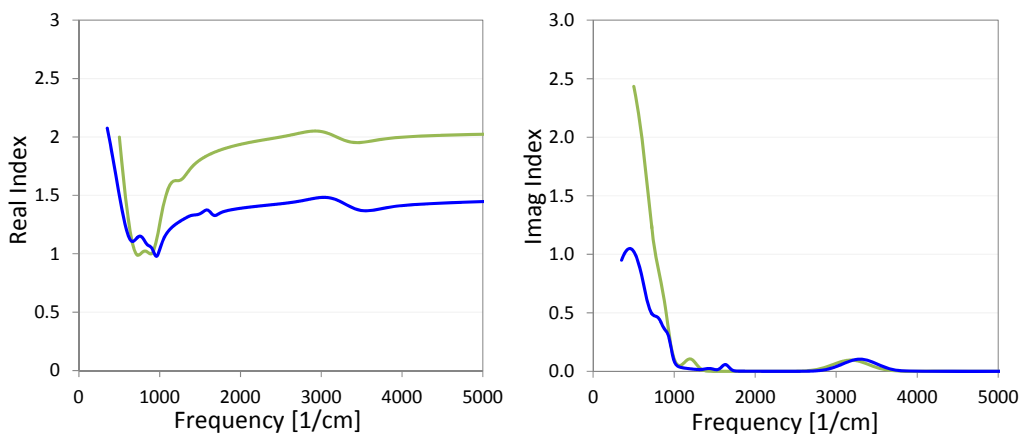


Figure 4. Refractive index corresponding to before (green) and after (blue) HF vapor exposure at a concentration of 30 ppm over 24 hours at ~30% RH.

3.2 Tag Exposure Systems

The gaseous exposure system (GES) was used to expose individual coated tags and other test pieces to a mixture of nitrogen, HF, and water vapor in a controlled and reproducible manner. A photograph of the complete GES exposure system is presented in Figure 5 (a). The system is based on commercial permeation sources (KIN-TEK), and gas flow or temperature adjustment is changed to alter the output HF concentration. The GES system provides an HF exposure using a flow of HF with dry nitrogen. Humidity was incorporated using a water bubbler and a static mixer. Adjusting the flow of dry nitrogen through a bubbler adjusts the vapor phase humidity of water seen by the sample under exposure. All of our exposure tests were performed under RH values ranging from 0-45%. Two different exposure fixtures were developed for the GES, a single tag exposure fixture and a multiple tag exposure fixture. A CAD model of one block of this multiple tag fixture is depicted in Figure 5 (b). HF exposure concentrations that can be achieved with the GES range from 1 to 40 ppm.

A headspace vapor exposure system (HVES) was also designed and implemented. The HVES approach provides a means of exposing tags to relatively high concentrations of the chemical (~10 – 500 ppm) for short periods of time, under very high humidity conditions (~100% RH). While our material studies indicated that exposures in the HVES resulted in more dramatic chemical reactions than observed in the GES (and the GES is more representative of the

envisioned implementation environment), the HVES data enabled exposure tests during realization of the GES and for testing that was outside of the operational constraints of the GES. The system consists of a small volume PVDF container; a schematic of the container is depicted in Figure 5 (c). A teflon block (not shown) is placed in the open volume of the container, and an chemical/water solution is poured around the block. The polarization tag is placed on top of the block to keep it out of contact with the liquid solution while exposing the tag to the surrounding atmosphere that contains a known concentration of chemical vapor.

For many of our initial tests, during which many tag coating materials were being tested, exposures were performed at HF concentrations of 30 ppm for a period of 1 day. Once promising results were obtained for these exposure conditions, the tag design would be tested under lower concentrations and longer periods of time. This exposure approach was used to identify the TiO₂ coating approach described in section 3.1 as the best approach for this system.

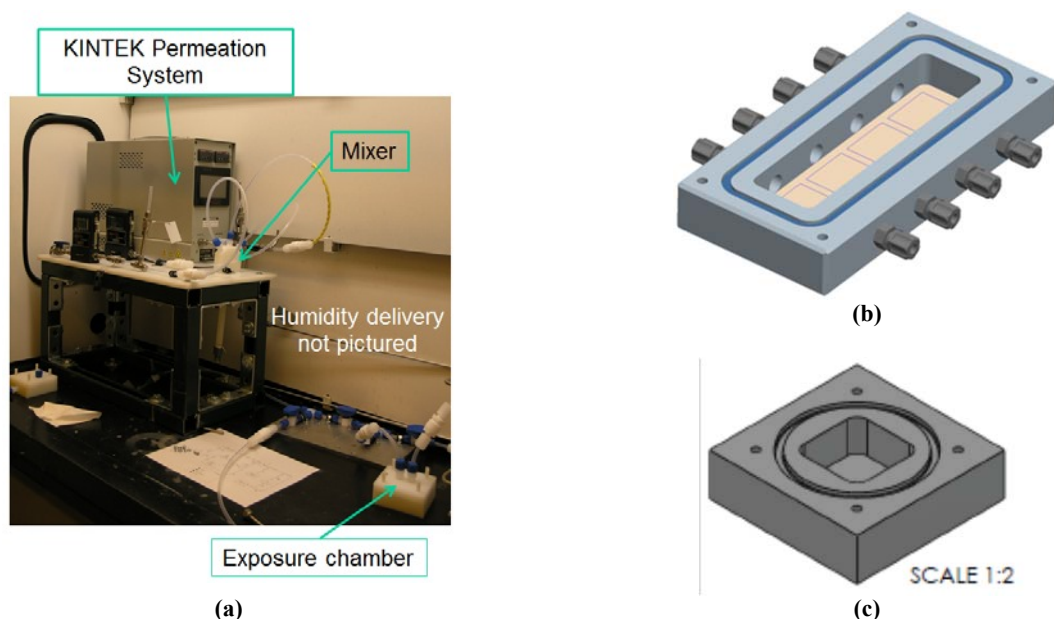


Figure 5. Gas exposure system (a) photograph, (b) CAD model of gas exposure test chamber, (c) CAD model of HVES test chamber.

3.3 Polarimeter Development

The second component of the chemical detection system is the polarimeter that measures the polarization properties of the light reflected off of the tags. During operational use, the data collected with the polarimeter would be used to determine if a tag had been exposed to HF during its monitoring period. However, for the development work presented here, the data collected by the polarimeter is used to quantify the sensitivity of the overall system, and ultimately whether or not the tags were exposed to a detectable quantity of HF.

Spectrally resolved Mueller matrix measurements were collected during tag development and testing to identify the spectral passbands over which substantial changes in the polarimetric behavior of the test tags were observed after exposure to HF gas. These measurements were focused over portions of the infrared optical spectrum for which uncooled detectors are commercially available and relatively inexpensive, namely the near infrared and short wavelength infrared (NIR and SWIR, or $\lambda = 0.9 - 2.3 \mu\text{m}$) and long wavelength infrared (LWIR, or $\lambda = 8.0 - 12.0 \mu\text{m}$). This data was collected in a monostatic measurement configuration with normal incident illumination and detection using an infrared Mueller matrix spectropolarimeter that has been described in detail elsewhere [11].

The primary quantity of interest derived from these Mueller matrix measurements is the linear diattenuation of the tags, defined as

$$D = \frac{\sqrt{m_{21}^2 + m_{31}^2}}{m_{11}}, \quad (4)$$

where the Mueller matrix elements are as defined in Eq. 1. Preliminary versions of the tags were characterized early in the development effort, and example diattenuation data for two such tags is depicted in Figure 6 (a). These tags were produced using a different coating technique [7] than was ultimately used for the final tag design; thus these tags served as a first estimate of tag performance. Linear diattenuation data acquired for the preliminary tags indicated that the longer wavelength region of the SWIR, namely $\lambda = 2.0 - 2.3 \mu\text{m}$, provided the most substantial and consistent change in linear diattenuation after exposure at a total dose of 30 ppm HF for 24 hours in the HVES. Consequently, all subsequent system development work focused on this passband. Diattenuation data for two of the final tag prototypes is presented in Figure 6 (b) for an exposure experiment of 20 ppm HF for 36 hours and 18% RH in the GES. The changes in diattenuation are notably less for the exposure experiments involving the final tag prototypes; however this is not surprising as the GES is a more realistic exposure environment that typically produces more subtle chemical changes versus the HVES.

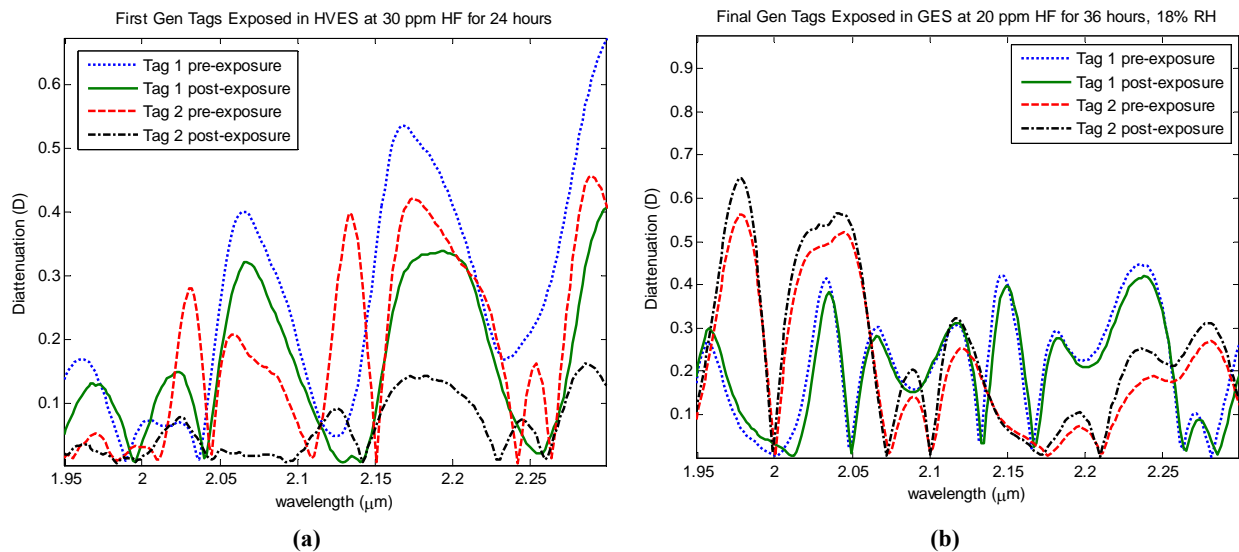


Figure 6. Diattenuation data derived from Mueller matrix measurements of (a) first generation tags exposed in the HVES, and (b) final generation tags exposed in the GES.

In order to demonstrate the system's overall field deployable capability and utility for monitoring in a variety of situations, the polarimeter should maximize field portability and ease of use. Imaging over $\lambda = 2.0 - 2.5 \mu\text{m}$ enables the use of non-cryogenically cooled cameras, and ultimately the design of a highly field portable device. The most feasible commercially available detector material is SWIR HgCdTe (MCT). A commercial off the shelf (COTS) thermo-electrically cooled (TEC) camera using this detector material offered by Photon Etc. (the Zephyr camera with a 320x256 pixel format, 30 μm pitch, and an operational passband of $\lambda = 0.8 - 2.5 \mu\text{m}$) was selected as the best COTS camera option for the polarimeter.

While a number of different measurement architectures were analyzed and assessed, the final design selected for the polarimeter was a rotating analyzer polarimeter due to its simplicity, ease of implementation, and straightforward data processing approach. By using a single rotating analyzer element, the complete linear polarization state of the tag can be characterized using a series of time sequential measurements, each acquired using the analyzing polarizer at a different angular orientation. The various intensity measurements are then combined to recover the S_0 , S_1 , and S_2 Stokes parameters.

The polarimeter was designed to image the tag targets at distances ranging from 0.5 to 10 meters. To meet the demands for this imaging system, a custom lens design was developed and realized to integrate with the COTS MCT detector and housing. A two-element design with a manual focus that uses zinc selenide elements with aspheric

surfaces was implemented. The imaging optics operate at $f/1.4$ and with an effective focal length of 100 mm. The lens elements are combined with an interchangeable set of spectral filters to narrow the passband to the desired range (Spectrogon filters, $\lambda_0 = 2140 \text{ nm}$, 2200 nm , 2360 nm , $\Delta\lambda \approx 100 \text{ nm}$), a high extinction ratio analyzing polarizer (Moxtek UBB01A) that rotates to collect the linear polarization measurements, and finally a second generating Moxtek polarizer that can be flipped in and out of the optical path to allow for polarized calibration measurements to be acquired. A schematic of the optical layout of the complete polarimeter system is depicted in Figure 7 (a). A CAD assembly schematic and a photograph of the assembled system are presented in Figure 7 (b).

To facilitate tag characterization in a laboratory environment while the field portable polarimeter was being developed, a simplified tag polarization testbed was also developed. Figure 8 presents the optical layout of the testbed. The testbed offers the same polarization data acquisition capabilities as the field portable sensor but was developed using COTS parts that were assembled on a laboratory optical breadboard. A collimated beam from a broadband Newport 50 W quartz tungsten halogen (QTH) lamp source was used to illuminate the tags for testing. The same spectral filters and polarizer elements used in the field portable polarimeter and described above were used. Finally, an InSb camera (FLIR SC6700) with a $f/2.5$ 50 mm effective focal length lens served as the imaging camera. Unless otherwise noted, all tag polarization data presented in this paper was acquired with this testbed system.

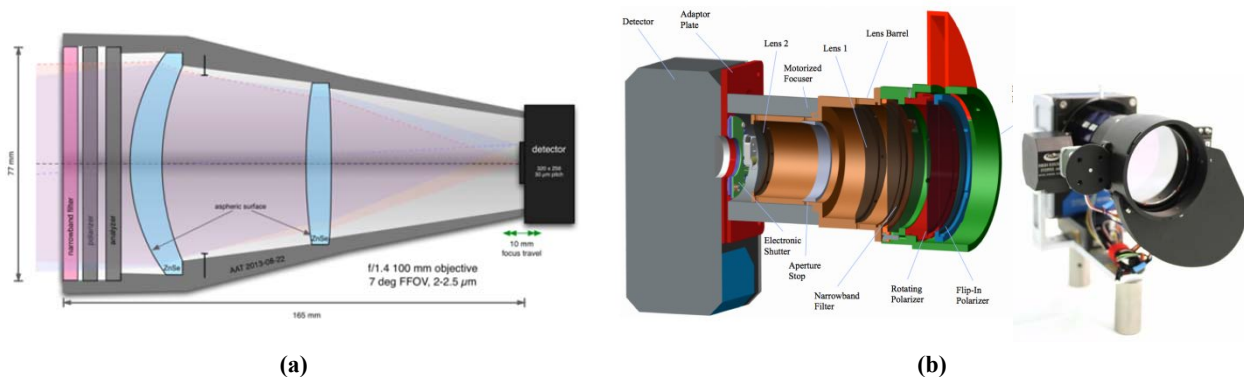


Figure 7: Rotating analyzer polarimeter (a) optical design layout, (b) assembly and photograph.

For all of the results presented in this report, the $DOLP$ values used to assess the tag capabilities are spatially averaged values, and the averaged $DOLP$ before and after exposure is the quantity that is compared. An empirical error analysis of the testbed polarimeter indicated that the measurement errors of the system could produce up to a ± 0.012 variation in the recovered spatially averaged $DOLP$ for a tag under test. Thus for the tag measurements presented in the following subsections, $DOLP$ changes must be greater than or equal to 0.025 to be assumed real and measurable changes.

3.4 Performance Assessment

To inform the system development effort, a radiometric system model was developed to predict the performance of the complete chemical monitoring system. The performance of the system was analyzed by calculating the system signal to noise ratio (SNR) and a receiver operator characteristic (ROC) curve for the cases of exposed and unexposed tags. The SNR and ROC analyses were implemented assuming the tag measurement methodology depicted in Figure 8. Light from the source propagates through the atmosphere, then reflects off the surface of the tag and propagates to the polarimeter, passing through the polarization analyzer, the imaging lens, and the spectral filter before reaching the detector. The system simulation was performed for a range of measurement distances $z = 0.5 - 10 \text{ m}$ from the tag, and a number of different optical $f/\#$ values. From these results, the illumination source and the specifications for the polarimeter's objective were derived.

The model assumes that the tags are illuminated by a broadband 60W QTH lamp source, and the atmospheric transmittance, $T_{\text{atm}}(z, \lambda)$, was modeled using MODTRAN to simulate the indoor horizontal air path using a room temperature of 72 deg F, 30% RH, and 880 mbar pressure. The tag component of the system model assumes that the tag is an ideal diattenuator of the specified percentage (ideal in the sense that there are no circular polarization

effects, birefringence, or depolarization properties). The Mueller matrix for a tag is simulated to be one of a diattenuator, and is described as a function of rotation angle (θ), maximum and minimum transmission (q and r), as [8]

$$M(q, r, \theta) = \frac{1}{2} \begin{bmatrix} q+r & (q-r) \cos 2\theta & (q-r) \sin 2\theta & 0 \\ (q-r) \cos 2\theta & (q+r) \cos^2 2\theta + 2\sqrt{qr} \sin^2 2\theta & (q+r-2\sqrt{qr}) \sin 2\theta \cos 2\theta & 0 \\ (q-r) \sin 2\theta & (q+r-2\sqrt{qr}) \sin 2\theta \cos 2\theta & (q+r) \sin^2 2\theta + 2\sqrt{qr} \cos^2 2\theta & 0 \\ 0 & 0 & 0 & 2\sqrt{qr} \end{bmatrix}. \quad (5)$$

Based on preliminary experimental results collected with exposed tags measured in the polarimetric testbed described in section 3.3, the tag is modeled as a 20% linear diattenuator before exposure and a 19.5% linear diattenuator after exposure (i.e. $D = \frac{q-r}{q+r} = 20\%$ or 19.5%). Additionally, the system model also assumes $q+r =$

1. Polarimetric calculations are done in units of 'fraction of flux', and this fractional data is then used to scale the in depth radiometric calculation.

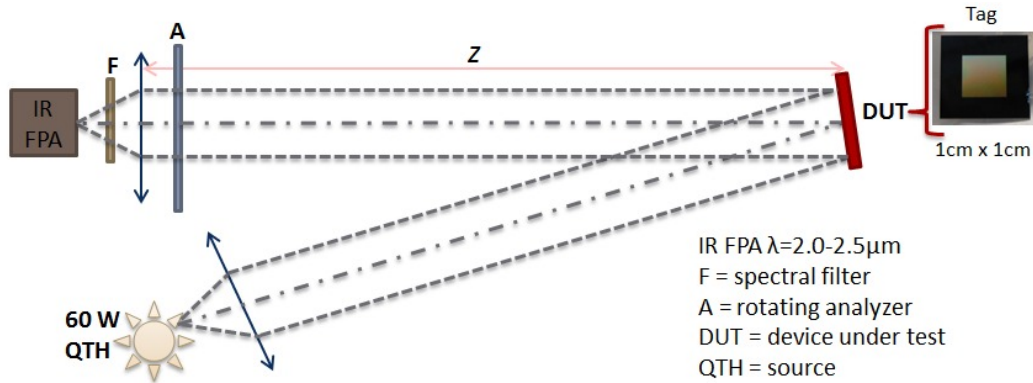


Figure 8. Layout of the optical system for the system model.

With respect to the polarimeter portion of the model, the imaging optics of the polarimeter are simulated using an ideal paraxial thin lens of fixed focal length. For the detector, FPA parameters from the Zephyr MCT camera were used. Since tag measurements occur over a relatively narrow spectral range, a 100 nm spectral filter centered at $\lambda = 2200$ nm was implemented in the model. Due to the availability of high quality wire grid polarizers, the polarization state analyzer is assumed to be an ideal polarizing element ($D = 1$ and extinction ratio, or ER, $= \infty$). For the purposes of the system model, the polarimetric imager is assumed to acquire imagery behind two analyzer configurations, both parallel and perpendicular to the thin fins that are incorporated in the tag's periodic structure.

To calculate the SNR for the system, the system model included all relevant noise sources, including shot noise, thermal noise, read noise, and dark current. Additionally, emissions from the tag were also incorporated into the simulation and treated as a noise term. The equation used to calculate the SNR is given by the ratio of the mean power of light received by the detector to the root sum squared (RSS) of the noises present, or

$$SNR(z, f/\#) = \frac{\tau_{\text{int}} QE \Phi(z, f/\#)}{\sqrt{\sum_1^n N_i^2}}. \quad (6)$$

In Eq. 6, τ_{int} is the integration time of the camera, QE is the quantum efficiency, Φ is the flux incident on a single FPA pixel, and the N_i are the noise terms in electrons. The flux is dependent on both the distance of the camera z as

well as the $f/\#$ of the optics. For all of the analyses in this paper, the distance of the source is assumed to be equal to the distance of the polarimeter, the integration time was assumed to be 5 ms, and the effective focal length (EFL) of the objective was 100 mm. The SNR and ROC results are depicted in Figure 9. These results indicate that for a relatively fast lens, $f/1.4$, the system can reliably detect the tag with an $\text{SNR} \geq 7$ for measurement distances ranging from 0.5 to 10 m, and effectively discriminate a change in the tag's diattenuation from 0.200 to 0.195.

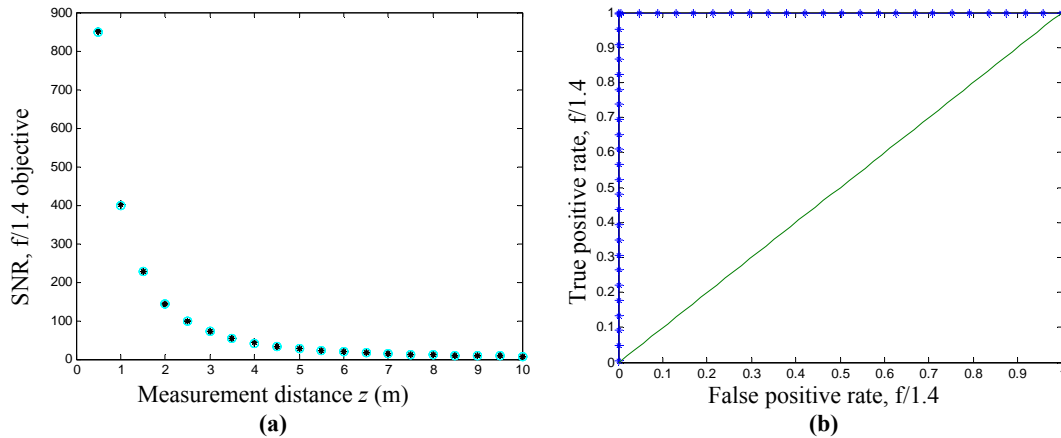


Figure 9. System model results using a 60 W QTH as the illumination source. (a) SNR versus distance, $f/\# = 1.4$. (b) ROC curve for a measurement distance of $z = 10$ m.

4. TESTING CONDITIONS AND RESULTS

4.1 Controlled Exposure Conditions

For many of the exposures performed to test the capabilities of the PChemS system, a relatively high concentration of HF was used (10-50 ppm). In contrast, industrial hygiene daily exposure limits for HF gas are substantially lower; for example OSHA lists the permissible exposure limit (PEL) as 3 ppm [12]. This exposure limit motivates that the tags be capable of detecting low concentrations of HF, and our envisioned implementation approach motivates that monitoring for that level be achievable over periods of weeks to months. However, testing all tags during our development efforts under low concentrations for extended periods is problematic from a feedback perspective. Exposing at higher concentrations allows for a quick learning environment where tags are exposed for time periods on the orders of days instead of months. Consequently, for many of our initial tests, during which many tag fabrication approaches were being tested, exposures were performed at 30 ppm for a period of 1 day. Once promising results were obtained for these exposure conditions, the tag design was tested under lower concentrations (≥ 1 ppm) and longer periods of time (1-30 days). Exposures were also performed under a variety of humidity levels (0-45% RH).

4.2 Controlled Exposure Results

To characterize the sensitivity of the PChemS detection system, the linear polarization properties of the light reflected off of a tag were measured before and after exposure by acquiring four intensity measurements at four analyzer orientations (0° , 45° , 90° , 135°) using the polarization testbed presented in section 3.3. During tag characterization, this data was acquired over the three different SWIR passbands afforded by the spectral filters. The linear Stokes parameters (S_0 , S_1 , and S_2) were then calculated, and the *DOLP* of the light reflected off the tag was calculated using Eq. 3. The resulting data product for a single exposure experiment is a set of intensity (S_0) and *DOLP* images. By comparing the *DOLP* before and after HF exposure, the detection capability of the system can be determined.

DOLP and intensity results for a few example tags exposed to different experimental conditions are depicted in Figure 10. Each row in the figure corresponds to a different tag under test, and the first column describes the exposure conditions. Intensity data is in arbitrary units. Spatially averaged *DOLP* values for the before and after exposure measurements are used to calculate a total change in *DOLP* ($\Delta DOLP$) experienced by the tag, and these values are provided in the last column of the table. All data presented in Figure 10 was acquired using the $\lambda_0 = 2200$ nm ($\Delta\lambda = 100$ nm) spectral filter; this filter narrowed the operational passband of the system to the spectral range

that most frequently produced a measurable $\Delta DOLP$ after exposure. For all example tags presented in Figure 10, a measurable change in $DOLP$ is observed, indicating that exposure of the tags to these conditions is detectable using our tag based detection system.

Typically, several tags were exposed to a given set of exposure conditions to enable repeatability of results to be assessed. Furthermore, many exposure experiments were repeated more than once. Consequently, over the period of testing hundreds of tags were exposed and characterized using this process; Table 1 summarizes the results of all exposure experiments performed using the final prototype tags and the GES system. The table is a matrix of exposure conditions with concentrations used corresponding to the columns, and humidity levels corresponding to the rows. Values in the cells represent the total exposure dose (ppm-hours) a set of tags was exposed to. Finally, color is used to indicate detectability limits; red, yellow, and green indicate that no, some, or all tags exposed to these conditions produced a measurable polarization change, respectively.

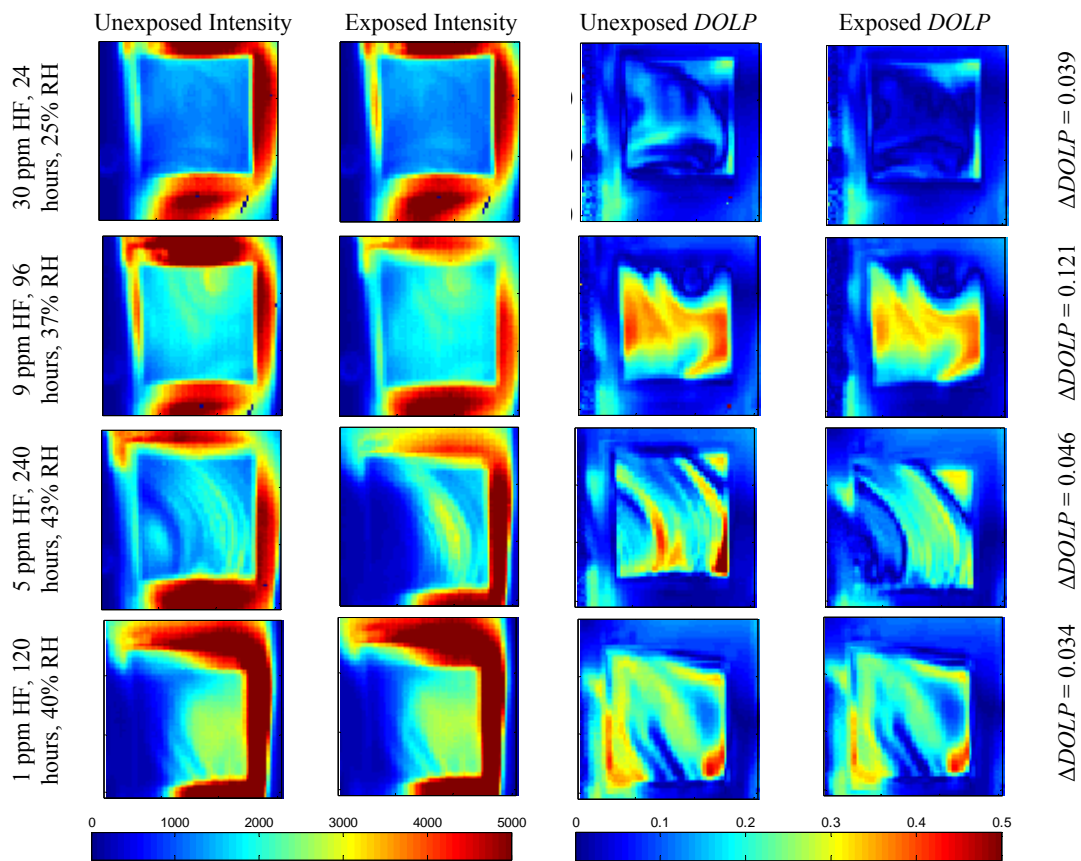


Figure 10. Example $DOLP$ results for the final generation of prototype tags, measured at $\lambda_0 = 2200$ nm and $\Delta\lambda = 100$ nm.

Overall, our objective was to establish limits with respect to the minimum detectable concentration of HF that could be detected by the system. In general, Table 1 indicates that higher concentrations of HF, and/or higher humidity values increased the likelihood that the system would detect the exposure. Furthermore, our experiments indicate concentrations as low as 1 ppm can be detected, provided the humidity during the exposure is adequate. In fact, humidity appears to play a key role in the success of the system; exposure experiments involving concentrations as high as 30 ppm yielded negative results without the presence of at least some humidity. Our material science work confirms that water vapor is essential to the reaction of the TiO_2 detector material with HF gas [9].

Table 1. Summary of exposure results for tags exposed in the gaseous exposure system. Values in the cells represent total exposure dose (ppm-hours).

		HF Concentration (ppm)							
		1	3	5	7	10	20		30
humidity (%RH)	0	-	-	-	-	-	-		720
	10	-	-	-	-	-	-		720, 2880
	17-23	720	-	-	-	-	120, 480	720 1440	720
	28-33	-	406	-	672		120, 480		-
	35-43	120	-	600	1200	336	372	960	120, 480
No detectable change				Some detectable change			Consistent detectable change		

4.3 Selectivity Testing and Results

The determination that the exposure of amorphous TiO₂ to HF gas produces a hydronium titanium oxyfluoride phase [9] is promising in that the phase contains fluoride and therefore the exact phase is unlikely to be generated by TiO₂ reaction with other species. However, the fact that it is a hydronium phase does raise the concern that similar reactivity may be observed on exposure to other acids. Thus an investigation of the selectivity of the deposited TiO₂ material to HF versus other acids, specifically hydrochloric (HCl) and nitric (HNO₃), was performed.

As with HF, the OSHA permissible exposure limits were the target concentration for exposure [12]. To avoid condensation problems that occur when these exposures are performed in the HVES, an open environment exposure was conducted by exposing the tags to the acids in an open container inside a vented chemical fume hood. The *DOLP* values of the tags used in these experiments, both before and after acid exposure, are depicted in Figure 11. For all tests, no measurable change in *DOLP* was found for any of the tags exposed. These results, though preliminary, indicate that the HF sensitivity of the TiO₂ coated tags is sufficiently selective, and thus we do not expect that exposure to other acids will produce a confounding measurable change in *DOLP*.

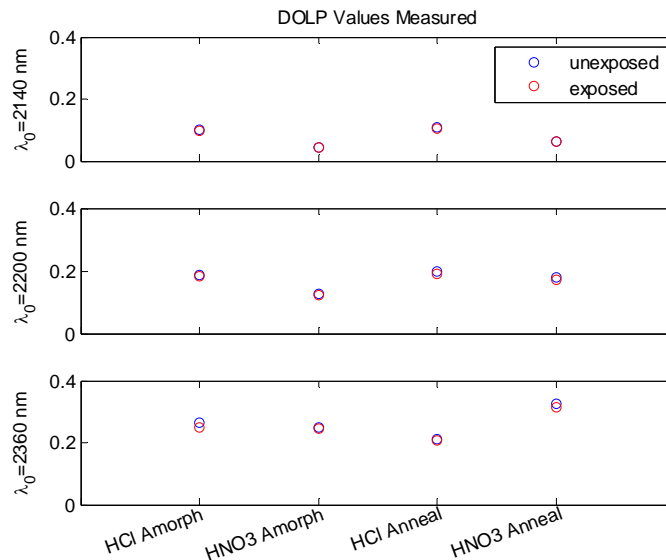


Figure 11. Spatially averaged *DOLP* results for tags exposed to different acids. Both amorphous and annealed 150 nm TiO₂ coatings were tested. None of these tags demonstrated a polarimetric change after exposure.

5. CONCLUSIONS AND PLANS FOR FUTURE WORK

In this paper we present on the development of and results from a proof-of-concept system that can be used for persistent HF gas monitoring. The system provides unique monitoring advantages over the current state of the art. Research under this effort included the design, development, and testing of a unique tag that experiences a change in optical polarization properties upon exposure to a chemical of interest, a polarimeter that can be used to interrogate the tag and determine if a measurable exposure occurred, and an exposure system for testing tags under controlled and characterized environments. Our results indicate that our current tag design approach is sensitive to HF concentrations as low as 1 ppm. Future work will include efforts to improve upon our existing tag design to offer a system that has improved sensitivity, selectivity, and robustness. Further development of a tag modeling capability to enable more accurate and comprehensive performance predictions is also planned.

In addition, although we focused our demonstration efforts on developing a system that was specifically sensitive to HF gas, the overall tag-based detection concept demonstrated here could be extended to other gases or vapors of interest.

6. ACKNOWLEDGEMENTS

This work was funded by the Department of Energy's National Nuclear Security Administration, Office of Defense Nuclear Nonproliferation Research & Development, Dr. Victoria Franques, Program Manager. Sandia National Laboratories is a multi-program laboratory managed and operated by Sandia Corporation, a wholly owned subsidiary of Lockheed Martin Corporation, for the U.S. Department of Energy's National Nuclear Security Administration under contract DE-AC04-94AL85000. SAND 2015-6546 C.

7. REFERENCES

- [1] F. Liang, T.L. Kelley, L. Luo, H. Li, M.J. Sailor, Y.Y. Li, "Self-Cleaning Organic Vapor Sensor Based on a Nanoporous TiO₂ Interferometer," *ACS Applied Materials & Interfaces*, 4 (8), 4177-4183,(2012).
- [2] S.E. Letant, M.J. Sailor, "Detection of HF Gas with a Porous Silicon Interferometer," *Advanced Materials*, 12 (5), 355-359 (2000).
- [3] B.J. Meulendyk, M.C. Wheeler, M.P. da Cunha, "Hydrogen Fluoride Gas Detection Mechanism on Quartz Using SAW Sensors," *IEEE Sensors Journal*, 11(9), 1768-1775 (2011).
- [4] J. Mertens, E. Finot, M.H. Nadal, V. Eyraud, O. Heintz, E. Bourillot, "Detection of gas trace of hydrofluoric acid using microcantilever," *Sensors and Actuators B-Chemical*, 99(1), 58-65 (2004).
- [5] Y.J. Tang, J. Fang, X.H. Xu, H.F. Ji, G.M. Brown, T. Thundat, "Detection of Femtomolar Concentrations of HF Using an SiO₂ Microcantilever," *Analytical Chemistry*, 76(9), 2478-2481 (2004).
- [6] R. R. Boye, C. M. Washburn, D. A. Scrymgeour, B. G. Hance, S. M. Dirk, D. R. Wheeler, W. G. Yelton, T. N. Lambert, "Development of an optically interrogated chemical tag," *Proc. SPIE 8024*, 80240A (2011).
- [7] C. M. Washburn, J. C. Jones, S. R. Vigil, P. S. Finnegan, R. R. Boye, J. D. Hunker, D. A. Scrymgeour, S. M. Dirk, B. G. Hance, J. M. Strong, L. M. Massey, M. T. Brumbach, "Flexible conductive polymer polarizer designed for a chemical tag," *Proc. SPIE 8613*, 861312 (2013).
- [8] D. Goldstein, [Polarized Light], 3rd Edition, Marcel Dekker, (2010).
- [9] L. Appelhans, P.S. Finnegan, L.T. Massey, T.S. Luk, M.A. Rodriguez, M.T. Brumbach, B. McKenzie, J. Craven-Jones, "Transformation of amorphous TiO₂ to a hydronium oxofluorotitanate and applications as an HF Sensor," in preparation for submission to *Sensor and Actuators B: Chemical*, 2015.
- [10] M. Estruga, M. Casas-Cabanas, D. Gutierrez-Tauste, C. Domingo, J.A. Ayllon, "Straightforward synthesis of a novel hydronium titanium oxyfluoride," *Materials Chemistry and Physics*, 124(2-3), 904-907 (2010).
- [11] D.H. Goldstein, D.B. Chenault, "Spectropolarimetric reflectometer," *Opt. Eng.* 41(5), 1013-1020 (2002).
- [12] Permissible exposure limits available at:
https://www.osha.gov/dts/chemicalsampling/toc/chmn_A.html